

The nuclear model with explicit mesons

We consider a nuclear model where the nucleus is held together by emitting and absorbing mesons, and the mesons are treated explicitly [?]. We are considering the regime of low-energy nuclear physics and this model is different from conventional interaction models in several ways. Firstly, the nucleons interact by emitting and absorbing mesons and not via a phenomenological potential. Conceptually this is similar to the one-boson-exchange model. Secondly, the number of parameters is greatly reduced. Regardless of the meson type, the number of parameters is two; the range and the strength of the meson-nucleon coupling are denoted b and S respectively. In the case of the pion, the central force, tensor force and the three-body force are all concealed within these two parameters. This model should be able to reproduce phenomena within the realm of low-energy nuclear physics such as the deuteron, nucleon-nucleon scattering, pion-nucleon scattering and pion photoproduction. The low energy regime also enables the use of the Schrödinger equation to describe the equations of motion. The model must be constructed in a way such that usual quantum numbers are conserved; this means conservation of isospin, angular momentum and parity.

1.1 Nuclear interacting model with explicit pions

In the following, we focus on the nuclear model with explicit pions. The pion is the lightest of the strongly interacting particles with a mass of about 15% of the nucleon mass. This yields a large Compton wavelength of 1.4 fm which means the longest contribution to nucleon-nucleon interactions. Furthermore, the pion is a significant component of the nuclear wave function where the pion dominates meson exchange corrections to different nuclear properties. In general, the bare nucleon is surrounded by several virtual pions. They are virtual in the same sense that the positron-electron pair are virtual in pair creation from a photon. It is important to stress the fact that these are virtual since they can have properties possible for true particles. The multi-component wave function of the nucleon can be written as

$$\Psi_N = \begin{bmatrix} \psi_N \\ \psi_{N\pi} \\ \psi_{N\pi\pi} \\ \vdots \end{bmatrix}, \quad (1.1)$$

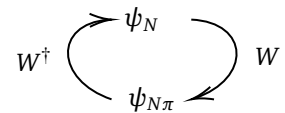


Figure 1.1: Illustration of the pion-nucleon operator, W

where ψ_N is the bare nucleon and the other wave functions are dressed by an arbitrary number of pions indicated by the subscripts. Assuming the nuclear interaction conserved isospin, angular momentum and parity we can construct the following operator for the pion-nucleon operator

$$W \equiv (\boldsymbol{\tau} \cdot \boldsymbol{\pi})(\boldsymbol{\sigma} \cdot \mathbf{r})f(r) \quad (1.2)$$

$$W^\dagger \equiv \int_V d^3r (\boldsymbol{\tau} \cdot \boldsymbol{\pi})^\dagger (\boldsymbol{\sigma} \cdot \mathbf{r})^\dagger f(r), \quad (1.3)$$

where $\boldsymbol{\tau}$ is the isovector of Pauli matrices acting on the nucleon in isospin space and $\boldsymbol{\sigma}$ is the same but for spin space and \mathbf{r} is the relative coordinate distance between the nucleon and the pion. These operators ensure the conservation of isospin, angular momentum and parity. The isovector of pions is denoted $\boldsymbol{\pi}$ and can be combined with $\boldsymbol{\tau}$ can be represented as a traceless 2-by-2 hermitian matrix given by

$$\boldsymbol{\tau} \cdot \boldsymbol{\pi} = \tau_0 \pi_0 + \sqrt{2} \tau_- \pi^+ \sqrt{2} \tau_+ \pi^- = \begin{bmatrix} \pi^0 & \sqrt{2} \pi^- \\ \sqrt{2} \pi^+ & -\pi^0 \end{bmatrix}, \quad (1.4)$$

where the isospin coefficients will be important later when we discuss different photoproduction processes. Similarly, by expanding the matrices in spin space and using the spherical tensor operator we get the following matrix in terms of the spherical harmonics

$$\boldsymbol{\sigma} \cdot \mathbf{r} = \sqrt{\frac{4\pi}{3}} r \begin{bmatrix} Y_1^0 & \sqrt{2} Y_1^{-1} \\ \sqrt{2} Y_1^1 & Y_1^0 \end{bmatrix}, \quad (1.5)$$

where similar to in isospin space, the off-diagonals include a factor $\sqrt{2}$.

There is also a phenomenological, short-range form factor $f(r)$ given by

$$f(r) = \frac{S}{b} e^{-r^2/b^2}, \quad (1.6)$$

where S and b are the pion-nucleon coupling strength and range respectively—these are illustrated in figure 1.2. The action of annihilating a pion must include the integral over coordinate space to remove the coordinate. We now have everything we need to construct a general Hamiltonian for the multi-component wave function of the nucleon in (1.1)

$$H = \begin{bmatrix} K_N & W^\dagger & 0 & \dots \\ W & K_N + K_\pi + m_\pi c^2 + V_C & W^\dagger & \dots \\ 0 & W & K_N + K_{\pi(1)} + K_{\pi(2)} + 2m_\pi c^2 + V_C & \dots \\ \vdots & \vdots & \vdots & \ddots \end{bmatrix}, \quad (1.7)$$

where the kinetic operators are given by

$$K_N = \frac{-\hbar^2}{2m_N c^2} \frac{\partial}{\partial \mathbf{R}^2} \quad (1.8)$$

$$K_\pi = \frac{-\hbar^2}{2m_\pi c^2} \frac{\partial}{\partial \mathbf{r}^2}. \quad (1.9)$$

Note the different derivatives—here \mathbf{R} is the center-of-mass coordinate and \mathbf{r} is the relative coordinate. The subscripts on the kinetic operators in (1.7) represent the order in which the pions are created. Should there be charged particles involved one must include a Coulomb interaction denoted by V_C . From (1.1) and (1.7) we can construct the general Schrödinger equation

$$H\Psi_N = E\Psi_N, \quad (1.10)$$

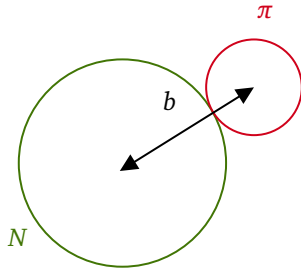


Figure 1.2: Schematic figure of the system to describe the form factor, (1.6). The pion is assumed to sit on the surface.

where the ground state is the bare nucleon surrounded by virtual pions. The ground state energy in the rest frame of the nucleon gives the mass of the physical nucleon. Within the framework of this model, one can generate a physical pion by supplying enough energy such that the pion is no longer virtual. The pion is trapped behind a potential barrier of height $m_\pi c^2 = 140$ MeV and cannot leave unless this or more energy is supplied to the system.

1.2 Dressing of the nucleon in the one pion approximation

We now consider the scenario where a photon interacts with the nucleon-pion systems and generates a physical pion. This means the energy is higher than the potential barrier also when taking recoil effects into account. This also hints at how a pion photoproduction process would emerge naturally as a disintegration process in this nuclear model. To generate more pions the photon energy would have to be increased by the same amount. This also means one could assume the first pion is responsible for the largest contribution to the nucleon dressing. This will be referred to as the one pion approximation. As a proof-of-concept we constrain ourselves to the one pion approximation and adding more pions should in principle be straight forward extension of the following calculations.

Returning to (1.1) and enforcing the one pion approximation yields

$$\Psi = \begin{bmatrix} \psi_N(\mathbf{R}) \\ \psi_{N\pi}(\mathbf{r}) \end{bmatrix}. \quad (1.11)$$

The Hamiltonian which acts on the two-component wave function in (1.11) is given by¹

$$H = \begin{bmatrix} K_N & W^\dagger \\ W & K_N + K_\pi + m_\pi c^2 \end{bmatrix}, \quad (1.12)$$

1. Strictly speaking one should use a three-component wave function to account for the mass difference between π^0 and π^\pm . This is done in appendix ??.

So far we have kept the model as simple as possible by expressing the equations in terms of the nucleon. From now on we treat the nucleon of two states of the same strongly interacting object with an intrinsic degree of freedom which defines the proton and neutron. We choose the proton and neutron as

$$|p\rangle = \begin{bmatrix} 1 \\ 0 \end{bmatrix} \quad |n\rangle = \begin{bmatrix} 0 \\ 1 \end{bmatrix}. \quad (1.13)$$

Furthermore, we denote the spin state of the nucleon by an arrow

$$\uparrow = \begin{bmatrix} 1 \\ 0 \end{bmatrix} \quad \downarrow = \begin{bmatrix} 0 \\ 1 \end{bmatrix}. \quad (1.14)$$

The wave function must also be normalized to one nucleon per unit volume. This is as far as we get in general terms for the dressing of the nucleon in the one pion approximation.

1.3 Dressing of the proton

We now focus our attention on the dressing of the proton in the spin-up state. The calculations are almost identical remembering the definitions

from section 1.2. The wave function of the bare proton can thus be written as

$$\psi_p = \frac{p \uparrow}{\sqrt{V}} \quad (1.15)$$

The Hamiltonian (1.12) suggest the following expression for the wave function of the pion-nucleon system

$$\psi_{N\pi} = (\boldsymbol{\tau} \cdot \boldsymbol{\pi})(\boldsymbol{\sigma} \cdot \mathbf{r}) \frac{p \uparrow}{\sqrt{V}} \phi(r), \quad (1.16)$$

where $\phi(r)$ is the radial function which will play an integral part in the rest of this section. From (1.2) we can construct the Schrödinger equation of the system

$$\begin{bmatrix} K_p & W^\dagger \\ W & K_N + K_\pi + m_\pi c^2 \end{bmatrix} \begin{bmatrix} \psi_p \\ \psi_{N\pi} \end{bmatrix} = E \begin{bmatrix} \psi_p \\ \psi_{N\pi} \end{bmatrix}. \quad (1.17)$$

Note that the kinetic operator in the second row still contains K_N to emphasise that this acts on the general nucleon-pion wave function, $\psi_{N\pi}$. Expanding (1.17) yields two equations

$$K_p \psi_p + W^\dagger \psi_{N\pi} = E \psi_p \quad (1.18)$$

$$W \psi_p + (K_N + K_\pi + m_\pi c^2) \psi_{N\pi} = E \psi_{N\pi}. \quad (1.19)$$

In the rest frame of the proton the center-of-mass dependency vanishes and inserting the operator (1.2) yields

$$\int_V d^3r (\boldsymbol{\tau} \cdot \boldsymbol{\pi})^\dagger (\boldsymbol{\sigma} \cdot \mathbf{r})^\dagger f(r) \phi(r) (\boldsymbol{\tau} \cdot \boldsymbol{\pi})(\boldsymbol{\sigma} \cdot \mathbf{r}) p \frac{1}{\sqrt{V}} = E p \frac{1}{\sqrt{V}}, \quad (1.20)$$

where the integration comes from equation (1.3). This can be further simplified using relations for the matrix vectors²

$$\begin{aligned} 2. \quad & (\boldsymbol{\tau} \cdot \boldsymbol{\pi})^\dagger (\boldsymbol{\tau} \cdot \boldsymbol{\pi}) = 3 \\ & \text{and } (\boldsymbol{\sigma} \cdot \mathbf{r})^\dagger (\boldsymbol{\sigma} \cdot \mathbf{r}) = r^2 \end{aligned}$$

$$12\pi \int_0^\infty dr f(r) \phi(r) r^4 = E. \quad (1.21)$$

Similarly for (1.19) where the term $K_N \psi_{N\pi}$ vanishes,

$$\begin{aligned} & (\boldsymbol{\tau} \cdot \boldsymbol{\pi})(\boldsymbol{\sigma} \cdot \mathbf{r}) f(r) p \frac{1}{\sqrt{V}} - \frac{\hbar^2}{2\mu_{N\pi}} \nabla_r^2 (\boldsymbol{\tau} \cdot \boldsymbol{\pi})(\boldsymbol{\sigma} \cdot \mathbf{r}) p \frac{1}{\sqrt{V}} \phi(r) \\ & = (E - m_\pi c^2) (\boldsymbol{\tau} \cdot \boldsymbol{\pi})(\boldsymbol{\sigma} \cdot \mathbf{r}) \phi(r) p \frac{1}{\sqrt{V}}, \end{aligned} \quad (1.22)$$

using (1.9) and where $\mu_{N\pi}$ is the reduced mass of the nucleon-pion system. This equation can be further simplified by using a vector operator relation which yields³

$$3. \quad \nabla^2(\mathbf{r}\phi(r)) = \mathbf{r} \left(\frac{d^2\phi(r)}{dr^2} + \frac{4}{r} \frac{d\phi(r)}{dr} \right)$$

$$f(r) - \frac{\hbar^2}{2\mu_{N\pi}} \left(\frac{d^2\phi(r)}{dr^2} + \frac{4}{r} \frac{d\phi(r)}{dr} \right) = (E - m_\pi c^2) \phi(r). \quad (1.23)$$

This means equation (1.21) and (1.23) are the two equations that must be solved numerically.

$$\left. \begin{aligned} & 12\pi \int_0^\infty dr f(r) \phi(r) r^4 = E \\ & f(r) - \frac{\hbar^2}{2\mu_{N\pi}} \left(\frac{d^2\phi(r)}{dr^2} + \frac{4}{r} \frac{d\phi(r)}{dr} \right) + m_\pi c^2 \phi(r) = E \phi(r) \end{aligned} \right\} \quad (1.24)$$

The bracket on the right is used to emphasise that (1.24) is a coupled system.

1.4 Numerical considerations

To solve the system of equations (1.24) one can consider two different numerical approaches. One approach gives a more intuitive picture of how to solve this kind of equation while the other is more robust and practical.

For a given E one can solve the second-order differential equation corresponding to $\phi[E]$. Conversely, for a given $\phi(r)$ one can calculate the integral to find $E[\phi]$. This leads to the fixed-point equation given by

$$E[\phi[\mathcal{E}]] = \mathcal{E}, \quad (1.25)$$

which is a single variable non-linear equation. Equation (1.25) can be solved using a root-finding algorithm. This approach is generally not as efficient since the algorithm will have to search through large parameter space to find a suitable solution.

The second approach consists of reformulating the system (1.24) as a boundary value problem with the following conditions

$$I'(r) = 12\pi f(r)\phi(r)r^4, \quad I(0) = 0, \quad I(\infty) = E. \quad (1.26)$$

Essentially, what is written in equation 1.26 is the boundary conditions we require for the energy. The equation starts from a singular point and extends to an infinite point. We require the solution to stay finite which means approximations are needed at both limits. At $r \rightarrow 0$ the differential equation is approximately an Euler-Cauchy equation with basis solutions 1 and r^{-1} . For finite solutions the latter is ignored which means $\phi'(a) = 0$ is the requirement for $a \approx 0$.⁴ For $r \rightarrow \infty$ the dominating term in the differential equation is

$$-\phi''(r) + 2\mu_{N\pi}(m_\pi c^2 - E)\phi(r) = 0. \quad (1.27)$$

Since we expect a negative value for E the basis solutions are on the form

$$\phi(r) = \exp\left\{\pm\sqrt{2\mu_{N\pi}(m_\pi c^2 + |E|)}r\right\}. \quad (1.28)$$

In the case of a positive sign, the solution diverges. For the basis solution with negative exponents, we have

$$\phi'(r) + \sqrt{2\mu_{N\pi}(m_\pi c^2 + |E|)}\phi(r) = 0. \quad (1.29)$$

These two conditions are suitable boundary conditions for the left and right boundaries, respectively. The algorithm converges and a solution to (1.17) is found. The solutions can be seen in figure 1.3 for the parameters $S = 10$ MeV and $b = 1$ fm.

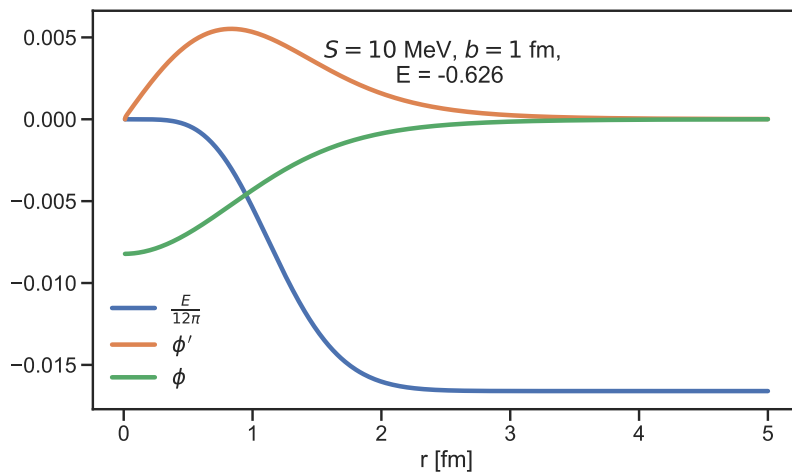


Figure 1.3: Boundary value problem solutions. The plot is generated using a tolerance of 10^{-6} . The blue line representing the energy is scaled.

4. You would end up with the same conclusion if you consider $\phi = a + r^n$ and plug this into $\phi'' + 4\phi'/r = 0$, which yields $n = 0, -1$.

Also, note that since we expect the energy to be less than zero it makes sense for the wave function to be negative since all other terms in the integral in equation (1.24) are positive. It might appear strange to have a negative wave function, $\phi(r)$ but there are two things to note. One can add an arbitrary phase to equation (1.11) and flip the sign. Also for all calculations, we are only interested in the norm-square of the wave function. The energy for the parameters shown in figure 1.3 is $E = -0.626$ MeV and this value is very sensitive to the parameters S and b since they enter in the form factor as seen in equation (1.6) and as mentioned in section 1.1 this gives the physical mass of the proton—it's importance will be clear later when comparing the discussion the mass contribution from virtual pion in section 2.

Since we cannot allow the wave function to extend to infinity numerically we must introduce some cut-off. Since the wave function of the pion-nucleon system has a built-in range parameter b it is natural to let the cut-off be proportional to this parameter. Within the regime of nuclear physics, we expect the wave function to extend up to a length within the order of magnitude of ten Fermi. Quantitatively this means a small constant of proportionality $O(0.01)$ in front of r_{\min} and another constant $O(1)$ in front of r_{\max} . Numerically, a constant of proportionality for r_{\max} and the impact can be seen on figure 1.4 where the radial wave functions stop after $5r_{\max}$.

Figure 1.4: Radial wave function for different parameters S and b to illustrate the behaviour on the radial function.

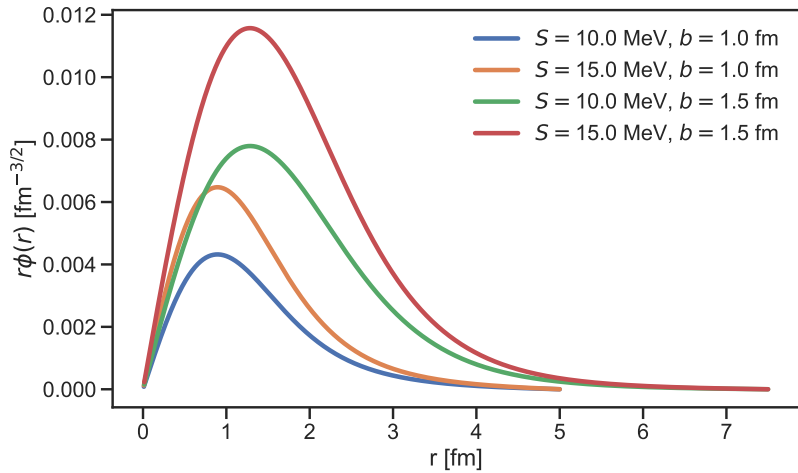


Figure 1.4 also illustrates the behaviour of the radial wave functions as the parameters change. As the coupling strength parameter S increases the radial wave function increases. As the range parameter b increases the peak is shifted to this new value. Also, note the unit of the radial wave function. We know the following integral must be dimensionless

$$\int_V d^3R \int_V d^3r |\psi_{N\pi}|^2, \quad (1.30)$$

which means the wave function $\phi(r)$ must have dimensions of $\text{fm}^{-5/2}$ and the radial wave function $r\phi(r)$ must have dimensions of $\text{fm}^{-3/2}$.

1.4.1 Different form factors

Compared to conventional interaction models of the nucleus this model has the advantage of having very few parameters. The phenomenological form factor $f(r)$ only consists of an interaction strength S and a range parameter b . Essentially all the complicated interactions from other

nuclear models are hidden in these two parameters and their behavior as a function of the nuclear length, r . We do, however, not know the exact way in which these are related and we must therefore make an educated guess. On figure 1.5 the same problem is solved as in 1.4 but the form factor is Yukawa-like, that is

$$f(r) = \frac{S}{b} \frac{\exp\{-1.4r\}}{r} \quad (1.31)$$

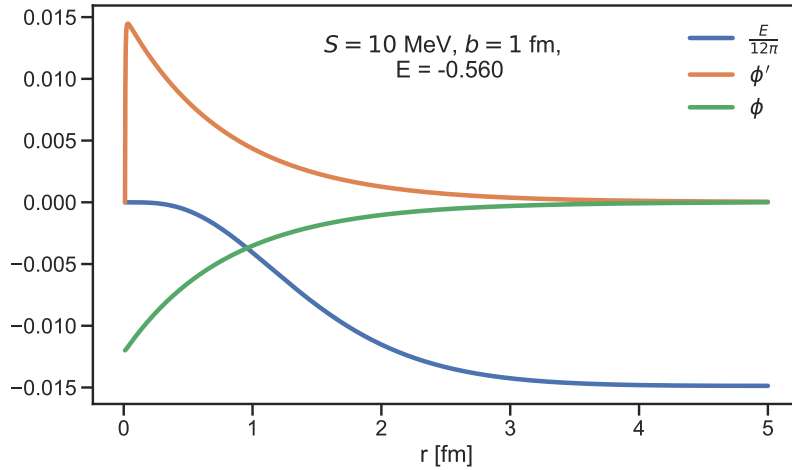


Figure 1.5: Boundary value problem solutions for a Yukawa-like form factor. The plot is generated using a tolerance of 10^{-6} . The RMS values of the relative residuals over each mesh intervals is shown in the Appendix. For clarity, the energy is scaled.

Note the scaling of the exponential is somewhat arbitrary.

1.4.2 Relativistic Expansion

It is customary to assume a nonrelativistic limit when considering regular quantum mechanics. To account for relativistic effects we can replace the kinetic term, K_r in (1.17)

$$K_r \rightarrow K_{r,rel} = \sqrt{p^2 c^2 + \mu_{N\pi}^2 c^4} = \mu_{N\pi} c^2 \left(\sqrt{1 + \frac{p^2}{\mu_{N\pi}^2 c^2}} - 1 \right), \quad (1.32)$$

where $\mu_{N\pi}$ is the reduced mass of the nucleon-pion system. This leads to a new systems of equations and these solutions can be compared found in the nonrelativistic limit to deduce with relativistic regime dominates the physical setup. More specifically we can compare the energy ratios denoted by E_R . Starting from (1.19)

$$f(r)(\boldsymbol{\tau} \cdot \boldsymbol{\pi})(\boldsymbol{\sigma} \cdot \mathbf{r})\psi_p + \mu_{N\pi} c^2 \left(\sqrt{1 + \frac{p^2}{\mu_{N\pi}^2 c^2}} - 1 \right) \psi_{N\pi} = (E - m_\pi c^2) \psi_{N\pi}, \quad (1.33)$$

This equation turns out to be divergent and we must therefor resort to an approximation. The kinetic energy is expanded

$$K_{r,rel} = \mu_{N\pi} c^2 \sqrt{1 + \frac{p^2}{\mu_{N\pi}^2 c^2}} - \mu_{N\pi} c^2 \approx \frac{p^2}{2\mu_{N\pi}} - \frac{p^4}{8\mu_{N\pi}^3 c^2} \quad (1.34)$$

This means we get an extra term in (1.22) yielding

$$f(r)\mathbf{r} - \left(\frac{p^2}{2\mu_{N\pi}} - \frac{p^4}{8\mu_{N\pi}^3 c^2} \right) \mathbf{r} \phi(r) = (E - m_\pi c^2) \mathbf{r} \phi(r) \quad (1.35)$$

Using the vector operators yields the following expression⁵

5.

$$\begin{aligned} \nabla^4(\mathbf{r}\phi(r)) &= \nabla^2(r\phi'' + 4\phi') \\ &= 2\phi'''' + 2(\nabla\phi'' \cdot \nabla)r + 4\phi''' \\ &= r\phi'''' + 6\phi''' \end{aligned}$$

$$f(r) - \frac{\hbar^2}{2\mu_{N\pi}} \left(\phi^{(2)}(r) + \frac{4}{r} \phi^{(1)}(r) \right) + \frac{\hbar^3}{8\mu_{N\pi}^3 c^3} \left(\phi^{(4)}(r) + \frac{6}{r} \phi^{(3)}(r) \right) = (E - m_\pi c^2) \phi(r), \quad (1.36)$$

where the exponent, (n) , is the order the differentiation. This leads to a system of equations given by

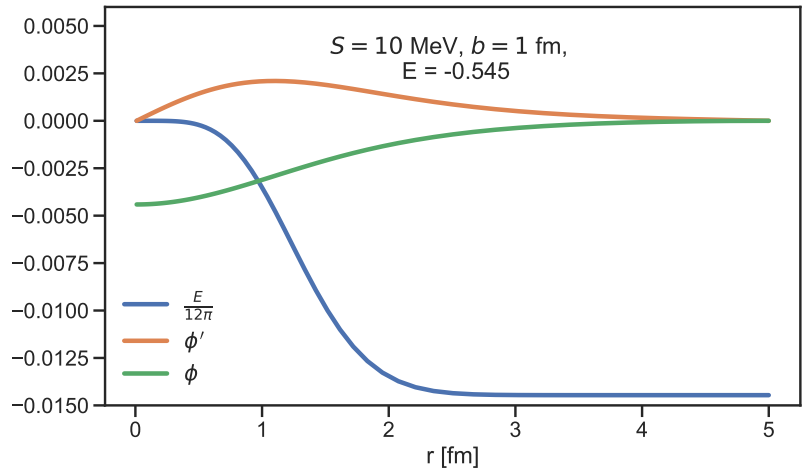
$$\left. \begin{aligned} 12\pi \int_0^\infty dr f(r) \phi(r) r^4 &= E \\ f(r) - \frac{\hbar^2}{2\mu_{N\pi}} \left(\phi^{(2)}(r) + \frac{4}{r} \phi^{(1)}(r) \right) + \frac{\hbar^3}{8\mu_{N\pi}^3 c^3} \left(\phi^{(4)}(r) + \frac{6}{r} \phi^{(3)}(r) \right) &= (E - m_\pi c^2) \phi(r) \end{aligned} \right\} \quad (1.37)$$

This system is a fourth order differential equation coupled to an integrodifferential equation and is solved using the boundary value problem technique. The boundary conditions can be found using the same considerations as in the previous section. For $r \rightarrow \infty$ the dominating terms are

$$\phi^{(4)}(r) = 8\mu_{N\pi}^3 (E - m_\pi c^2) \phi^{(1)}(r) + 4\mu_{N\pi} \phi^{(2)}(r) \quad (1.38)$$

The solutions are shown in figure 1.6

Figure 1.6: Boundary value problem solutions for the relativistic expansion. The plot is generated using a tolerance of 10^{-3} . The energy convergence is scaled.



Since we ultimately want to get values for S and b it is nice to get some intuition behind the behavior of the solutions as we vary these two parameters. This is shown in figure 1.7.

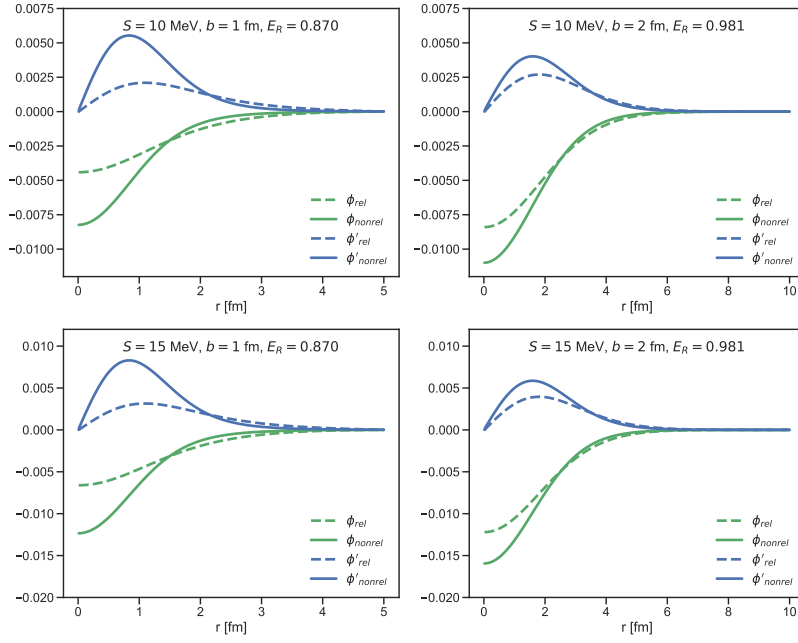


Figure 1.7: Plots for different values of the parameters S and b to illustrate the difference between the nonrelativistic equations and the relativistic equations.

From figure 1.7 one can also deduce the effect of changing the parameters S, b . Increasing the parameter b will flatten the wavefunction which will decrease the energy. This corresponds to increasing the distance between the pion and the nucleus. Increasing the coupling strength S will increase the amplitude of the wave function. In (1.6) we assumed a form but this could might as well be an exponential or even Yukawa-like. We should keep in mind that this form factor greatly impacts the behavior of the system; both in relation to the boundary conditions and the length scale of the wave function.

Pion photoproduction

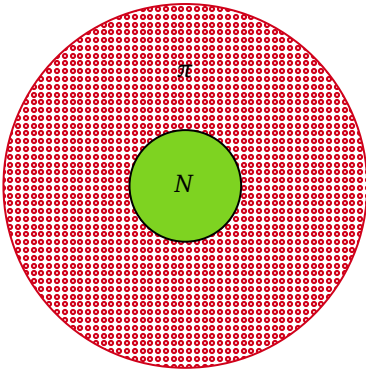


Figure 2.1: Illustration of the dressed nucleon. In the centre (green) is a nucleon and surrounding it is a cloud of virtual pions (red gradient).

We now consider the case of pion photoproduction. In the model mentioned in section 1.1 the nucleon is in a superposition of states with an arbitrary number of pions. We can write a general multicomponent wavefunction of the nucleon as

$$\Psi_N = \begin{bmatrix} \psi_N \\ \psi_{N\pi} \\ \psi_{N\pi\pi} \\ \vdots \end{bmatrix}, \quad (2.1)$$

where ψ_p is the wave function of the isolated nucleon and $\psi_{N\pi}$ is a system consisting of the nucleon and one pion and the same logic applies to the different wavefunctions. We will refer to the systems with one or more pions as dressed nucleon states in the sense that the isolated nucleon is dressed by a cloud of virtual pions—this is illustrated in figure 2.1. It is important to stress the fact that these are virtual pions. This means in order to generate a pion some energy $m_\pi c^2 \approx 140$ MeV must be added to the system. Within this framework, pion photoproduction comes naturally through photodisintegration. In other words, we disintegrate the nucleon-pion system and create pions in the process. More specifically we disintegrate a two-body system and this is photoproduction within the framework of this model. The disintegration approach is inspired by another two-component system, the deuteron. We, therefore, expect the same approach to apply here. Deuteron photodisintegration is covered in Appendix ???. We consider an initial (bound) state given by

$$|\Phi_i\rangle = \begin{bmatrix} \phi_p \\ \phi_{N\pi} \end{bmatrix}, \quad (2.2)$$

where ϕ represents a bound state. The final state consists of the same superposition but in an unbound system represented by ψ , i.e.

$$|\Psi_f\rangle = \begin{bmatrix} \psi_p \\ \psi_{N\pi} \end{bmatrix}. \quad (2.3)$$

Note that we only consider one-pion systems since we expect this to be largest contribution to the dressed nucleon—nonetheless this is an approximation.

2.0.1 Normalization of the initial state

We must also impose some normalization. Starting from (2.2)

$$\Phi = \mathcal{N} \begin{bmatrix} p \uparrow \\ (\boldsymbol{\tau} \cdot \boldsymbol{\pi})(\boldsymbol{\sigma} \cdot \mathbf{r}) p \uparrow \phi(r) \end{bmatrix}, \quad (2.4)$$

where \uparrow represents the spin state, $\phi(r)$ is the wavefunction from figure 1.3 and \mathcal{N} is the normalization constant. This leads to

$$\langle \Phi | \Phi \rangle = |\mathcal{N}|^2 (\langle \phi_p | \phi_p \rangle + \langle \phi_{N\pi} | \phi_{N\pi} \rangle) \quad (2.5)$$

$$= |\mathcal{N}|^2 (V + 3V \int d^3r r^2 \phi(r)^2) \quad (2.6)$$

$$\stackrel{!}{=} 1. \quad (2.7)$$

This leads to the following normalization constant

$$\mathcal{N} = \frac{1}{\sqrt{V}} \frac{1}{\sqrt{1 + \epsilon}}, \quad (2.8)$$

where V is the volume and ϵ is the integral in (2.6). To figure out what particle can be knocked out by a photon via photodisintegration we consider the pion channel in (2.3). This expression is the properly normalized initial state.

2.0.2 Normalization of the final state

The final state consists of the unbound system represented by ψ . Expanding the terms using the isospin operators yields¹

$$\phi_{N\pi} = c(\boldsymbol{\tau} \cdot \boldsymbol{\pi})(\boldsymbol{\sigma} \cdot \mathbf{r})p \uparrow \phi(r) = c(p\pi^0 + \sqrt{2}n\pi^+)(\boldsymbol{\sigma} \cdot \mathbf{r}) \uparrow \phi(r). \quad (2.9)$$

From this equation, the first result should be highlighted. We consider two photodisintegration processes

$$p\gamma \rightarrow p\pi^0 \quad (2.10)$$

$$p\gamma \rightarrow n\pi^+, \quad (2.11)$$

where due to orthogonality of the states in isospin space the process involves the neutron is proportional to $\sqrt{2}$. Since this term will exist throughout the calculations we know the ratio between these two processes must be related by a factor of 2. There are also some corrections related to the mass difference between the proton and the neutron. This will be evident when comparing the matrix elements in section 2.0.3.

This expansion will be useful when evaluating matrix elements with the different spin states represented by $(\uparrow\downarrow)$. Considering the final state which consists of a plane wave. It is useful to expand this in terms of spherical harmonics. Using the spherical harmonic decomposition of the plane wave yields

$$\frac{1}{\sqrt{V}} e^{-i\mathbf{q} \cdot \mathbf{r}} = \frac{1}{\sqrt{V}} \sum_{\ell, m} 4\pi i^\ell Y_\ell^{*m}(\mathbf{q}) Y_\ell^m(\mathbf{r}) j_\ell(qr) \quad (2.12)$$

$$= \frac{1}{\sqrt{V}} \sum_{\ell} 4\pi i^\ell j_\ell(qr) \left(\frac{2\ell + 1}{4\pi} \right) P_\ell(\cos \theta), \quad (2.13)$$

where θ is the angle between \mathbf{q} and \mathbf{r} also illustrated on 2.2 and P_ℓ is the Legendre polynomial of degree ℓ . For now \mathbf{q} is some variable related to the energy of the photon and will act as momentum. This is illustrated on figure 2.3 and is expanded upon in the next section. Also, the spherical harmonic addition theorem has been used.² Since we are considering the pion channel just above the threshold we do the following expansion

$$\frac{1}{\sqrt{V}} e^{i\mathbf{q} \cdot \mathbf{r}} \stackrel{\ell=0}{=} \frac{1}{\sqrt{V}} j_0(qr), \quad (2.14)$$

which is assumed to be the dominant contribution

$$1. \tau_0\pi^0 + \sqrt{2}\tau_+\pi^- + \sqrt{2}\tau_-\pi^+$$

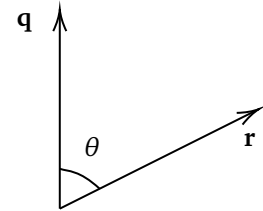


Figure 2.2: Illustration of the angle between the two vectors \mathbf{q} and \mathbf{r} in equation (2.14)

$$2. \sum_m Y_\ell^m(\mathbf{p}') Y_\ell^{*m}(\mathbf{r}) = \left(\frac{2\ell+1}{4\pi} \right) P_\ell(\cos \theta)$$

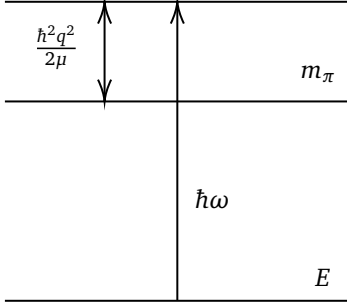


Figure 2.3: Illustration of the energy levels. Here the energy E refers to the energy shown in 1.3 and will act as a zero-point energy.

2.0.3 Photoproduction: dipole approximation

Having properly normalized the initial and final states we now move on to the actual matrix element we want to calculate. As the normalization of the final state suggests we limit ourselves to dipole transitions. This is an approximation and constraints the cross section to only be correct for low energies. In order works this should only apply for photon energies just above the threshold. We now want to calculate the matrix element in within the dipole approximation, that is

$$\langle \Psi_f | \mathbf{d} | \Phi_i \rangle, \quad (2.15)$$

where \mathbf{d} is the dipole operator, $|\Phi_i\rangle$ and $|\Psi_f\rangle$ are given by (2.2) and (2.3) respectively. As before, we only consider the pion channel. Since we are considering transitions just above the threshold we only consider the contributions from the electric dipole term. This terms is assumed to dominate and higher order terms can be calculated later if necessary. Considering the pion channel for the following process $p\gamma \rightarrow n\pi^+$

$$\mathcal{M} = -i\omega_k \sqrt{\frac{2\pi\hbar}{V\omega_k}} \mathbf{e}_{\mathbf{k},\lambda} \langle \frac{1}{\sqrt{V}} e^{i\mathbf{q}\cdot\mathbf{r}} n\pi^+(\uparrow\downarrow) | \mathbf{d} | (\boldsymbol{\tau} \cdot \boldsymbol{\pi})(\boldsymbol{\sigma} \cdot \mathbf{r}) p \uparrow \phi(r) N \rangle \quad (2.16)$$

where the two arrows represent the two spin states of the neutron and the proton. Also, q is illustrated in figure 2.3 where the energy, E , is the same as in (1.24). This is the zero point energy in the system we are considering and can be written as

$$\frac{\hbar^2 q^2}{2\mu_{N\pi}} = \hbar\omega - m_\pi c^2, \quad (2.17)$$

where $\mu_{N\pi}$ is the reduced mass of the nucleon-pion system. Compare this equation to (??). The front factor arises from the quantization of the electromagnetic field. Using the results from section 2.0.2 and section 2.0.1. The different spin states of the neutron in the final state yields to contributions to the total matrix element given by

$$\mathcal{M}^\uparrow = \frac{-iN\sqrt{2}\omega_k \mathbf{e}_{\mathbf{k},\lambda}}{V} \sqrt{\frac{2\pi\hbar}{V\omega_k}} \langle j_0(qr) | d_0 r_0 | \phi(r) \rangle \quad (2.18)$$

$$= \frac{-iN\sqrt{2}\omega_k \mathbf{e}_{\mathbf{k},\lambda}}{V} \sqrt{\frac{2\pi\hbar}{V\omega_k}} \sqrt{\frac{4\pi}{3}} \langle j_0(qr) | d_0 r Y_1^0 | \phi(r) \rangle \quad (2.19)$$

$$\mathcal{M}^\downarrow = \frac{-iN2\omega_k \mathbf{e}_{\mathbf{k},\lambda}}{V} \sqrt{\frac{2\pi\hbar}{V\omega_k}} \langle j_0(qr) | d r_+ | \phi(r) \rangle \quad (2.20)$$

$$= \frac{-iN2\omega_k \mathbf{e}_{\mathbf{k},\lambda}}{V} \sqrt{\frac{2\pi\hbar}{V\omega_k}} \sqrt{\frac{4\pi}{3}} \langle j_0(qr) | d_0 r Y_1^1 | \phi(r) \rangle, \quad (2.21)$$

$$(2.22)$$

where the spin down state picks up a factor $\sqrt{2}$ from equation 1.5. Now

we calculate the remaining matrix elements,

$$\langle j_0(qr)|d_0r_0|\phi(r)\rangle = \frac{\mu}{m_\pi} e \langle j_0(qr)|r_0r_0|\phi(r)\rangle \quad (2.23)$$

$$= \frac{\mu}{m_\pi} e \frac{4\pi}{3} \langle j_0| r^2 |\phi(r)\rangle \quad (2.24)$$

$$= \frac{\mu e}{m_\pi} \int_0^\pi \int_0^{2\pi} \int_0^\infty dr d\phi d\theta j_0(qr) r^4 \cos^2 \theta \sin \theta \phi(r) \quad (2.25)$$

$$= \frac{4\pi\mu e}{3m_\pi} \underbrace{\int_0^\infty dr j_0(qr) r^4 \phi(r)}_{Q(r)}, \quad (2.26)$$

where the dipole operator has been inserted and the angular integrals calculated. Similarly for the next matrix element,

$$\langle j_0(qr)|d_{-r_+}|\phi(r)\rangle = \frac{\mu}{m_\pi} e \langle j_0(qr)|r_{-r_+}|\phi(r)\rangle \quad (2.27)$$

$$= \frac{4\pi\mu e}{3m_\pi} \langle j_0(qr)|r^2 Y_1^{-1} Y_1^1 |\phi(r)\rangle \quad (2.28)$$

$$= \frac{4\pi\mu e}{3m_\pi} Q. \quad (2.29)$$

This leads to the two final expressions for the two matrix elements

$$|\mathcal{M}^\uparrow| = \left(\frac{4\pi\mu e}{3m_\pi} \right)^2 \frac{2\mathcal{N}^2 \omega_k (2\pi\hbar)}{V^2} (\mathbf{e}_{\mathbf{k},\lambda})^0 (\mathbf{e}_{\mathbf{k},\lambda}^*)^0 Q^2 \quad (2.30)$$

Similarly for the next matrix element

$$|\mathcal{M}^\downarrow| = \left(\frac{4\pi\mu e}{3m_\pi} \right)^2 \frac{4\mathcal{N} \omega_k (2\pi\hbar)}{V^2} (\mathbf{e}_{\mathbf{k},\lambda})^+ (\mathbf{e}_{\mathbf{k},\lambda}^*)^+ Q^2. \quad (2.31)$$

Calculating the total matrix element using a polarization theorem³

$$|\mathcal{M}|^2 = |\mathcal{M}^\uparrow|^2 + |\mathcal{M}^\downarrow|^2 \quad (2.32)$$

$$= \frac{2\pi\hbar\omega_k \mathcal{N}^2 e^2}{V^2} \left(\frac{4\pi\mu}{3m_\pi} \right)^2 Q^2, \quad (2.33)$$

which is the final expression for the matrix element. According to Fermi's golden rule we can calculate the transition probability

$$d\omega = \frac{2\pi}{\hbar} |\mathcal{M}|^2 d\rho, \quad (2.34)$$

where the density of states is given by

$$d\rho = \frac{V q m}{\hbar^2 (2\pi)^3} d\Omega. \quad (2.35)$$

This is related to the differential cross section

$$\frac{d\sigma}{d\Omega_q} = \frac{16\pi}{9} \mathcal{N}^2 \alpha \frac{k q \mu_{N\pi}^3}{m_\pi^2 \hbar c} Q^2, \quad (2.36)$$

3. $(\mathbf{e}_{\mathbf{k},\lambda}^* \cdot \mathbf{e}_{\mathbf{k},\lambda}) = \delta_{\lambda,\lambda'}$ and $\mathbf{e}_{\mathbf{k},\mp} = \pm \frac{1}{\sqrt{2}} (\mathbf{e}_{\mathbf{k},1} \pm i\mathbf{e}_{\mathbf{k},2})$. This leads to $(\mathbf{e}_{\mathbf{k},\lambda}^{0*} \cdot \mathbf{e}_{\mathbf{k},\lambda'}^0) + (\mathbf{e}_{\mathbf{k},\lambda}^{0+} \cdot \mathbf{e}_{\mathbf{k},\lambda'}^+) = \delta_{\lambda,\lambda'} + \frac{1}{2} \delta_{\lambda,\lambda'}$

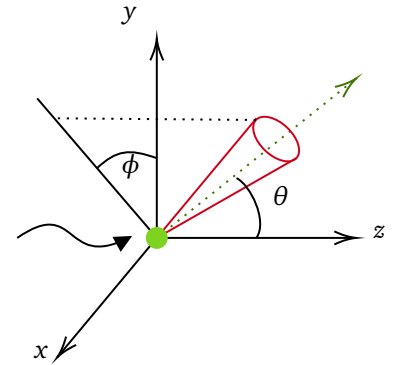


Figure 2.4: Illustration of the differential cross section.

and since there is no explicit angular dependency the total cross section is given by

$$\sigma_{\text{dipole}} = \oint_{4\pi} \frac{d\sigma}{d\Omega_q} d\Omega_q \quad (2.37)$$

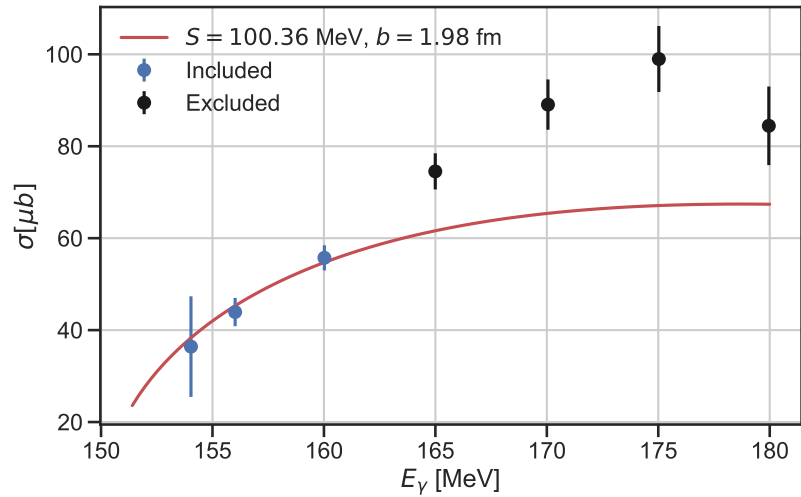
$$= 4\pi \frac{16\pi}{9} \mathcal{N}^2 \alpha \frac{kq\mu_{N\pi}^3}{m_\pi^2 \hbar c} Q^2 \quad (2.38)$$

$$= \frac{64\pi^2}{9} \mathcal{N}^2 \alpha \frac{kq\mu_{p\pi}^3}{m_\pi^2 \hbar c} \left(\int_0^\infty dr j_0(qr) r^4 \phi(r) \right)^2. \quad (2.39)$$

This is the final expression for the total cross section of photoproduction of charged pions using the dipole approximation. We now perform a fit to experimental data for the parameters S and b and enter in the wave function $\phi(r)$. Here two considerations are needed. Both the dipole approximation and the one-pion approximation limit the validity of the cross section to near threshold. And due to the limited amount of experimental data for charged pion photoproduction the fit is limited to approximately 15 MeV from the threshold. This means some data points are excluded to constrain the fitted parameters to values that might seem physically realistic.

The fit is performed and can be seen on figure 2.5.

Figure 2.5: The total cross section of the photoproduction process $\gamma p \rightarrow \pi^+ n$ fitted to experimental data. The fit parameters are shown in the figure. The blue data points are included in the fit and the black data points are excluded since these violate both the dipole and the one pion approximation.



The parameters S and b seem reasonable but more importantly we are interested in the relative weight coming from the $N\pi$ component in the wave function and the virtual pions contribution to the dressed proton. This corresponds to solving the equations in (1.24) with the new parameters. The contribution to the wave function is calculated as follows

$$\int_V d^3R \int_V d^3r |\psi_{N\pi}|^2 = 4\pi \int_0^\infty dr \phi(r)^2 r^2 \quad (2.40)$$

$$= 0.69 \quad (2.41)$$

using (??) and considering only the π^+ component in π . The energy is calculated which yields

$$E_{\text{virtual pions}} = -449 \text{ MeV}. \quad (2.42)$$

Note here that we have used two approximations that limit (2.39) to energies very close to the threshold. To further test the validity of the

model we need a more general expression for the cross section and more data points. This means we have to consider the exact matrix element for the transition and consider the photoproduction of neutral pions off protons since this is the most experimentally investigated photoproduction process.

2.1 Pion Photoproduction exact

In section ?? we looked at how to use the model described in section 1.1 to get an expression for the cross-section which was compared to experimental data. More specifically we used the dipole approximation which introduces a trade-off between the difficulty of the calculations and the regime in which our solution is valid. We expect the dipole approximation to hold for low energies just above the threshold. To both validate and generalize this result we now do a different approach and calculate the cross-section exact and also consider recoil effects. Strictly speaking, recoil effects should also be considered in section ?? since the mass ratio between the nucleon and the pion cannot be assumed to yield a stationary nucleon after the pion photoproduction process. To calculate the exact matrix elements we consider a non-relativistic system of particles interacting with the electromagnetic field. The interacting part of the Hamiltonian is given by

$$H = \frac{1}{2m_\pi} \left(\mathbf{p} - \frac{e}{c} \mathbf{A}(\mathbf{r}) \right)^2, \quad (2.43)$$

where \mathbf{p} is the momentum operator and $\mathbf{A}(\mathbf{r})$ is the quantized vector potential at the point \mathbf{r} . Note that we have already replaced the usual mass by the mass of the pion, m_π since we are considering the interaction of a pion with charge e with the electromagnetic field.

The electromagnetic interaction is relatively weak compared to the strong force. For our problem, this means we can expand the interaction by taking only the lowest non-vanishing order of perturbation into account. Since we later want to consider transition probabilities we only keep the first non-linear term of (2.43) which yields

$$V^{(1)} = -\frac{e}{2m_\pi c} \left(\mathbf{p} \cdot \mathbf{A}(\mathbf{r}_p, t) + \mathbf{A}(\mathbf{r}_p, t) \cdot \mathbf{p} \right), \quad (2.44)$$

which also means the interacting part is linear in the creation(annihilation) operators corresponding to single-photon emission(absorption). Our choice of gauge is purely conventional and we choose the radiation gauge which imposes a condition on the vector potential given by

$$\nabla \cdot \mathbf{A} = 0, \quad (2.45)$$

and this is a convenient choice of gauge since the commutator in (2.44) is $\nabla \cdot \mathbf{A}$ and we can write

$$V^{(1)} = -\frac{e}{m_\pi c} \mathbf{A}(\mathbf{r}_p, t) \cdot \mathbf{p}_p. \quad (2.46)$$

Note that (2.46) consists of the pion momentum operator, \mathbf{p}_π and the electromagnetic vector potential at a distance r_π . This distance was also mentioned in section 1.1 and can be expressed in term of the Jacobi coordinates illustrated on figure 2.6 where the relative coordinate is given by $\mathbf{r} = \mathbf{r}_\pi - \mathbf{r}_p$ which leads to the following transformation of equation (2.46)

$$V^{(1)} = -\frac{e}{m_\pi c} \mathbf{A}(\mathbf{r}_p, t) \cdot \mathbf{p}_p = -\frac{e}{m_\pi c} \mathbf{A} \left(\mathbf{R} - \frac{m_\pi}{M_{p\pi}} \mathbf{r}, t \right) \left(\frac{m_p}{M_{p\pi}} \mathbf{P} - \mathbf{p} \right), \quad (2.47)$$

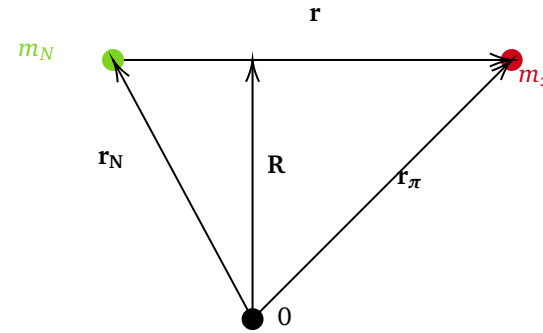


Figure 2.6: Jacobi coordinates illustrating \mathbf{r}_π used in the vector potential in equation 2.46. Here we use $\mathbf{r} = \mathbf{r}_\pi - \mathbf{r}_p$ and see that $\mathbf{r}_\pi = \mathbf{R} + \mathbf{r} \frac{m_p}{M_{p\pi}}$, where $M_{p\pi} = m_p + m_\pi$.

where $M_{p\pi} = m_p + m_\pi$ is the total mass of the system and \mathbf{R} is the coordinate vector for the center of mass. We now move on from the general theory of the pion interacting with the electromagnetic field and consider the specific case of pion photoproduction. To recap we consider the following processes

$$p\gamma \rightarrow p\pi^0 \quad (2.48)$$

$$p\gamma \rightarrow n\pi^+ \quad (2.49)$$

$$n\gamma \rightarrow n\pi^0 \quad (2.50)$$

$$n\gamma \rightarrow p\pi^-, \quad (2.51)$$

where the initial states consist of a dressed proton or neutron and a plane wave photon which in the language of 2nd quantization can be written as $a_{\mathbf{k},\lambda}^\dagger |0\rangle$ corresponding to creating a photon with wave vector \mathbf{k} and polarization λ from the vacuum $|0\rangle$. The final states consists of a nucleon and a pion and no photon, i.e electromagnetic vacuum. This leads to the following expression for the matrix element for the transitions in (2.48), (2.49), (2.50) and (2.51)

$$\frac{-e}{m_\pi c} \langle 0 | \mathbf{A}(\mathbf{R} - \frac{m_\pi}{M_{p\pi}} \mathbf{r}, t) a_{\mathbf{k},\lambda}^\dagger | 0 \rangle = \frac{-e}{m_p} \sqrt{\frac{2\pi\hbar}{\omega_{\mathbf{k}} V}} \mathbf{e}_{\mathbf{k},\lambda} e^{i\mathbf{k}(\mathbf{R} - \frac{m_\pi}{M_{p\pi}} \mathbf{r}) - i\omega_{\mathbf{k}} t}. \quad (2.52)$$

Completely analogous to section 2.0.3 and specifically equation (2.34) we now want to consider the probability of transition per unit time of going from the initial state $|i\rangle$ to $|f\rangle$ according to Fermi's golden rule

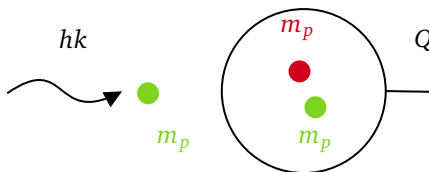
$$d\omega = \frac{2\pi}{\hbar} |\mathcal{M}|^2 d\rho, \quad (2.53)$$

where $d\rho$ is the density of states also analogous to (2.35). The difference is that we do not employ the dipole approximation to evaluate the matrix element \mathcal{M} and we also consider recoil. In the following section we focus on pion photoproduction of neutral pion off protons corresponding to the transition in (2.48). The choice is due to the fact that there is a lot more experimental data available for pion photoproduction off protons compared to neutrons since it is easier to achieve experimentally. We focus on neutral pions since our one-pion approximation is assumed to be valid near the threshold and since we are interested in fitting to experimental data we need as much data near the threshold as possible—and this is the case for neutral pion photoproduction

2.1.1 Neutral Pion Photoproduction off Protons

From (2.52) we get

$$\mathcal{M}^{(\uparrow\downarrow)} = \frac{e}{m_p} \sqrt{\frac{2\pi\hbar}{\omega_{\mathbf{k}} V}} \langle (\uparrow\downarrow) p\pi^0 | \frac{e^{i\mathbf{q}\cdot\mathbf{r}}}{\sqrt{V}} \frac{e^{i\mathbf{Q}\cdot\mathbf{r}}}{\sqrt{V}} | e^{i\mathbf{k}(\mathbf{R} - \frac{m_\pi}{M_{p\pi}} \mathbf{r})} (\mathbf{e}_{\mathbf{k},\lambda} \mathbf{p}) | (\boldsymbol{\tau} \cdot \boldsymbol{\pi})(\boldsymbol{\sigma} \cdot \mathbf{r}) \phi(r) \frac{p^\uparrow}{\sqrt{V}} \rangle \quad (2.54)$$



$$= \frac{-e}{m_p} \sqrt{\frac{2\pi\hbar}{\omega_{\mathbf{k}} V}} \langle (\uparrow\downarrow) \frac{e^{i\mathbf{q}\cdot\mathbf{r}}}{\sqrt{V}} \frac{e^{i\mathbf{Q}\cdot\mathbf{r}}}{\sqrt{V}} | e^{i\mathbf{k}(\mathbf{R} - \frac{m_\pi}{M_{p\pi}} \mathbf{r})} (\mathbf{e}_{\mathbf{k},\lambda} \mathbf{p}) | (\boldsymbol{\sigma} \cdot \mathbf{r}) \phi(r) \frac{\uparrow}{\sqrt{V}} \rangle, \quad (2.55)$$

Figure 2.7: Neutral pion photoproduction with conservation of momentum $\mathbf{k} = \mathbf{Q}$ illustrated

where we have used $\int d^3r e^{i\mathbf{k}\cdot\mathbf{R}} = V$ and $\langle p\pi^0 | \boldsymbol{\tau} \cdot \boldsymbol{\pi} | p \rangle = 1$. Note that \mathbf{q} is the wave-number of the pion-proton relative momentum and \mathbf{Q} is originates from conservation of momentum, that is $\mathbf{Q} = \mathbf{k}$. Defining a

new vector, $\mathbf{s} = \mathbf{q} + \frac{m_\pi}{M_{p\pi}} \mathbf{k}$ yields

$$\mathcal{M}^{(\uparrow\downarrow)} = \frac{-e}{m_\pi} \sqrt{\frac{2\pi\hbar}{\omega_k}} \frac{1}{V} \langle (\uparrow\downarrow) | \langle e^{i\mathbf{s}\cdot\mathbf{r}} | (\mathbf{e}_{\mathbf{k},\lambda} \mathbf{p}) (\boldsymbol{\sigma} \cdot \mathbf{r}) | \phi(r) \rangle | \uparrow \rangle \quad (2.56)$$

Note the different inner products. We now do the plane wave expansion using (2.12) and consider the angular averaging of two coordinates variables⁴

$$\langle e^{i\mathbf{s}\cdot\mathbf{r}} | (\mathbf{e}_{\mathbf{k},\lambda} \frac{\partial}{\partial \mathbf{r}}) (\boldsymbol{\sigma} \cdot \mathbf{r}) | \phi(r) \rangle = +i(\mathbf{e}_{\mathbf{k},\lambda} \cdot \mathbf{s}) \int d^3r e^{i\mathbf{s}\cdot\mathbf{r}} (\boldsymbol{\sigma} \cdot \mathbf{r}) \phi(r) \quad (2.57)$$

$$= -i(\mathbf{e}_{\mathbf{k},\lambda} \cdot \mathbf{s}) \int d^3r 3ir j_1(sr) \frac{\mathbf{s} \cdot \mathbf{r}}{sr} (\boldsymbol{\sigma} \cdot \mathbf{r}) \phi(r) \quad (2.58)$$

$$= (\mathbf{e}_{\mathbf{k},\lambda} \cdot \mathbf{s}) (\boldsymbol{\sigma} \cdot \mathbf{r}) \underbrace{\frac{4\pi}{s} \int_0^\infty dr r^3 j_1(sr) \phi(r)}_{F(s)} \quad (2.59)$$

$$= (\mathbf{e}_{\mathbf{k},\lambda} \cdot \mathbf{s}) (\boldsymbol{\sigma} \cdot \mathbf{r}) F(s). \quad (2.60)$$

Returning to the matrix element (2.55)

$$\mathcal{M}^{(\uparrow\downarrow)} = \frac{ie\hbar}{m_p} \sqrt{\frac{2\pi\hbar}{\omega_k}} \frac{1}{V} \langle (\uparrow\downarrow) | (\mathbf{e}_{\mathbf{k},\lambda} \cdot \mathbf{s}) F(s) | \uparrow \rangle \quad (2.61)$$

$$= \frac{ie\hbar}{m_p} \sqrt{\frac{2\pi\hbar}{\omega_k}} \frac{1}{V} (\mathbf{e}_{\mathbf{k},\lambda} \cdot \mathbf{s}) \langle (\uparrow\downarrow) | (\boldsymbol{\sigma} \cdot \mathbf{r}) | \uparrow \rangle F(s), \quad (2.62)$$

which leads to the following expression for the norm square⁵

$$|\mathcal{M}^{(\uparrow\downarrow)}|^2 = \frac{2\pi\hbar^3 e^2}{m_p^2 \omega_k V^2} |\mathbf{e}_{\mathbf{k},\lambda} \cdot \mathbf{s}|^2 |\langle (\uparrow\downarrow) | (\boldsymbol{\sigma} \cdot \mathbf{r}) | \uparrow \rangle|^2 F(s)^2, \quad (2.63)$$

and now calculating

$$\sum_\lambda |\mathbf{e}_{\mathbf{k},\lambda} \cdot \mathbf{s}|^2 = \sum_\lambda (\mathbf{e}_{\mathbf{k},\lambda}^* \cdot \mathbf{s}) (\mathbf{e}_{\mathbf{k},\lambda} \cdot \mathbf{s}) \quad (2.64)$$

$$= s^2 - \frac{(\mathbf{k} \cdot \mathbf{s})^2}{k^2} \quad (2.65)$$

$$= q^2 - \frac{(\mathbf{k} \cdot \mathbf{q})^2}{k^2} \quad (2.66)$$

$$= q^2 \sin^2(\theta_q), \quad (2.67)$$

where θ_q is the angle between \mathbf{k} and \mathbf{q} and we now have an angular dependency originating from the dot product. I have added a subscript q to empathize that this relative to the final state momentum \mathbf{q} located in (θ, ϕ) also illustrated on figure 2.4.

Plugging (2.64) into (2.63) yields

$$\frac{1}{2} \sum_{\lambda, (\uparrow\downarrow)} |\mathcal{M}_{fi}|^2 = \frac{\pi e^2 \hbar^3}{V^2 m_p^2} \frac{1}{\omega_k} q^2 \sin^2(\theta) s^2 F(s)^2. \quad (2.68)$$

According to Fermi's golden rule the transition probability is given by

$$d\omega = \frac{2\pi}{\hbar} |\mathcal{M}|^2 d\rho, \quad d\rho = \frac{V \mu_{p\pi} q}{\hbar^2 (2\pi)^3} d\Omega_q, \quad (2.69)$$

4. $\int d\Omega n_k n_l = \frac{4\pi}{3} \delta_{kl}$, which means $\int d\Omega r_k r_l = \frac{4\pi r^2}{3} \delta_{kl}$, where \mathbf{n} is a unit vector

5. We do this step already to use a completeness relation for the polarization.

where the density of states in the final state assumes a non-relativistic expansion. Strictly speaking this is an approximation. Also, \mathbf{q} denotes the differential angle element to empathize that this is relative to the pion-proton system. Plugging (2.68) into (2.69)

$$d\omega = \frac{e^2}{8\pi} \frac{\mu_{p\pi} c^2}{m_p^2 c^4 \omega_k} q^3 \sin^2(\theta_q) s^2 F(s)^2 d\Omega_q \quad (2.70)$$

which leads to the following expression for the differential cross section by considering the time it takes the photon to cross the volume, V .

$$\frac{d\sigma}{d\Omega_q} = \frac{e^2}{8\pi} \frac{M_{p\pi} c^2}{m_p^2 c^4} \frac{q^3}{k} \sin^2(\theta_q) s^2 F(s)^2 \quad (2.71)$$

In (2.71) we have an expression for the angular dependency. This means for some photon energy we get an angular distribution. This can also be compared to experimental data. (This can be done for all the figures in [?] and also for charged pions). Figure 2.8 shows the differential cross section as a function of the angle θ_{cm} compared to experimental data.

Figure 2.8: Not fitted parameters! Note the dependency is not $\sin(\theta_q)^2$ since there is a contribution from $F(s)$ as well.

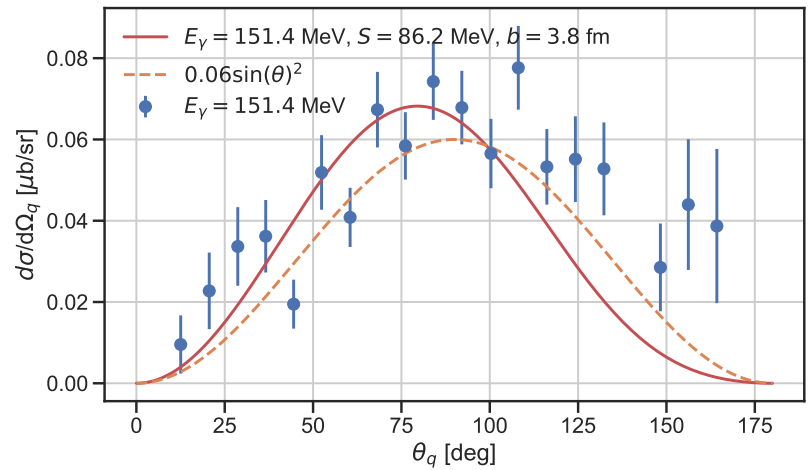
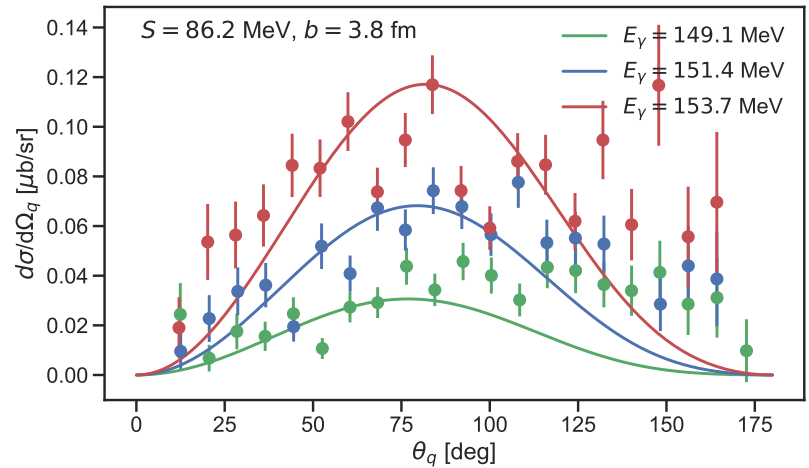


Figure 2.9: Multiple energies



To get an expression for the total cross section equation the expression

is integrated into containing only a radial part using

$$\sigma = 2\pi \int_0^\pi d\theta \sin(\theta_q) \frac{d\sigma}{d\Omega_q} \quad (2.72)$$

$$= 2\pi \int_0^\pi d\theta \frac{e^2}{8\pi} \frac{\mu_{p\pi} c^2}{m_p^2 c^4} \frac{q^3}{k} \sin^3(\theta) s^2 F(s)^2 \quad (2.73)$$

(2.72) is fitted to experimental data such that the physical parameters in our model S and b can be extracted. So far the values of these parameters have been chosen at random. However, we do have some intuition about how these two affect the wavefunction of the system from figure 1.7. From (2.72) we see that the wave function only enters explicitly in the integral so the general behavior of the cross section is hard to predict. The fit is done and can be seen in figure 2.10. Data is from [?]

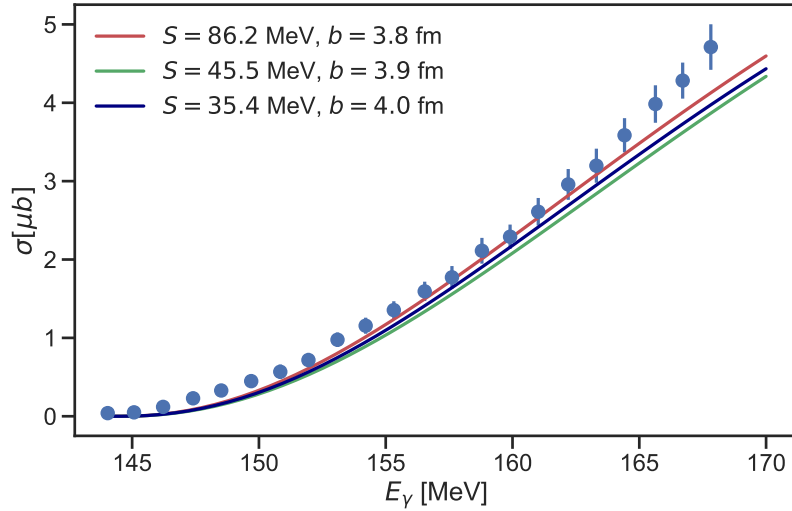


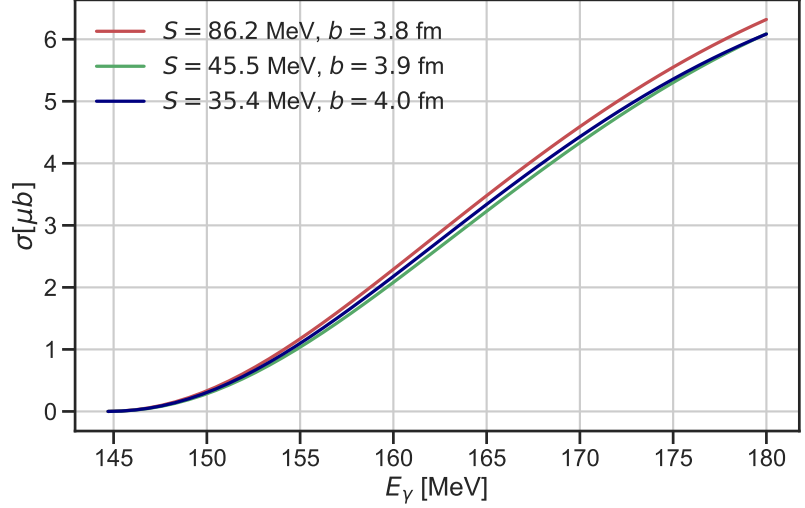
Figure 2.10: Fitted parameters to experimental data for the process $\gamma p \rightarrow \pi^0 p$. The fit parameters for S, b are shown inside the figure.

Note that these expressions are for the production of neutral pions. The same approach can be done for charged pions.

There is some freedom of choice in the fit. The integral is slowly converging and a cut-off must be introduced. This cut-off is arbitrary and does affect the fit. For a larger cut-off the line flattens out before 165 MeV. This leads to a more phenomenological discussion of the model in relation to the cross section as a function of energy. For higher energies we expect more than one pion to contribute to the cross section. This model, however, only takes one pion into account. To describe the behavior at higher energies more pions must be taking into account. This highlights the strengths and weaknesses of using differential equations to describe the physical system. If we take more pions into account this approach is no longer favorable since this leads to too many coupled systems. For more pions one would have to resort to another method.

For neutral pion off neutrons

Figure 2.11: The process $\gamma n \rightarrow \pi^0 n$ with the same parameters as for neutral pion photoproduction off protons.



2.2 Nuclear Effective Field Theory operator

The construction of the most general chiral Lagrangian is based on the theory of the non-linear realization of a symmetry. The baryon-number-conserving chiral Lagrangian can be split into pieces with even numbers of fermion fields where in this section we will focus on

$$\mathcal{L} = N^\dagger \left(i\mathcal{D}_0 + \frac{\mathcal{D}^2}{2m_N} \right) N + \frac{g_A}{2f_\pi} N^\dagger \boldsymbol{\tau} N \cdot \mathbf{D}\boldsymbol{\pi}, \quad (2.74)$$

where the second term is very similar to the creation operator W from equation (1.2)—only the \mathbf{r} is replaced by $\nabla_{\mathbf{r}}$. The general operator is constructed in such a way that parity, isospin and spin is conserved and there is some freedom in the choice of the distance operator. In this section we explore the differences, if any, by constructing the nuclear model with explicit mesons with the operator as is it defined in chiral effective field theory. We assume the following form of the wave function of the proton and the system consisting of a nucleon and a single pion

$$\psi_p = p \uparrow \frac{1}{\sqrt{V}}, \quad \psi_{N\pi} = (\boldsymbol{\tau} \cdot \boldsymbol{\pi})(\boldsymbol{\sigma} \cdot \frac{\partial}{\partial \mathbf{r}}) p \uparrow \frac{1}{\sqrt{V}} \phi, \quad (2.75)$$

where $\boldsymbol{\tau}$ and $\boldsymbol{\sigma}$ are vectors consisting of Pauli matrices acting on isospin and spin space on the nucleon respectively. $\boldsymbol{\pi}$ is the isovector of pions. We now construct an operator to create and annihilate a pion

$$W = (\boldsymbol{\tau} \cdot \boldsymbol{\pi})(\boldsymbol{\sigma} \cdot \frac{\partial}{\partial \mathbf{r}}) f(r) \quad (2.76)$$

$$W^\dagger = \int_V d^3r (\boldsymbol{\tau} \cdot \boldsymbol{\pi})^\dagger (\boldsymbol{\sigma} \cdot \frac{\partial}{\partial \mathbf{r}})^\dagger f(r), \quad (2.77)$$

where $f(r)$ is a form factor. The annihilation operator must contain the integral to remove the coordinate of the pion. This leads to the following Schrödinger equation

$$\begin{bmatrix} K_{\mathbf{R}} & W^\dagger \\ W & K_{\mathbf{R}} + K_{\mathbf{r}} + m_\pi c^2 \end{bmatrix} \begin{bmatrix} \psi_p \\ \psi_{N\pi} \end{bmatrix} = E \begin{bmatrix} \psi_p \\ \psi_{N\pi} \end{bmatrix}, \quad (2.78)$$

which is expanded

$$12\pi \int_0^\infty dr \frac{\partial^2}{\partial r^2} r^2 f(r) \phi(r) = E \quad (2.79)$$

$$\frac{\partial}{\partial r} f(r) - \frac{2\hbar^2}{\mu_{N\pi}} \frac{\partial^3}{\partial r^3} \phi(r) = (E - m_\pi c^2) \frac{\partial}{\partial r} \phi(r). \quad (2.80)$$

Assume the form factor is on the following form

$$f(r) = \frac{S}{b} e^{-r^2/b^2} \quad (2.81)$$

which yields

$$\frac{\partial}{\partial r} f(r) = \frac{-2r}{b^2} f(r), \quad \frac{\partial^2}{\partial r^2} = -\frac{2(b^2 - 2r^2)}{b^4} f(r). \quad (2.82)$$

The terms inside the integral in equation (2.79)

$$\frac{\partial^2}{\partial r^2} (r^2 f(r) \phi(r)) = 2r f(r) \phi(r) + 2r f'(r) \phi(r) + r^2 f(r) \phi'(r) \quad (2.83)$$

$$+ 2r f'(r) \phi(r) + r^2 f''(r) \phi(r) + r^2 f'(r) \phi'(r) \quad (2.84)$$

$$+ 2r f(r) \phi(r) + r^2 f'(r) \phi'(r) + r^2 f(r) \phi''(r) \quad (2.85)$$

$$\equiv Y(r) \quad (2.86)$$

Considering the limits of (2.80) which for large r is

$$-\frac{2\hbar^2}{\mu_{N\pi}} \phi'''(r) = (E - m_\pi c^2) \phi'(r) \quad (2.87)$$

The solution is shown on 2.12

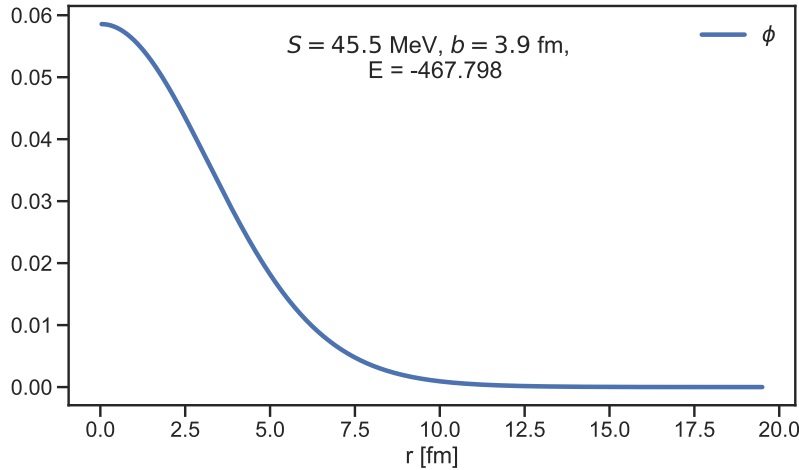


Figure 2.12: Fitted parameters to experimental data. The fit parameters for S, b are shown inside the figure.